Scientific Research Publishing

Journal of Modern Physics, 2022, 13, 918-931
https://www.scirp.org/journal/jmp
ISSN Online: 2153-120X
ISSN Print: 2153-1196

Harmony Is Cause—Not Consequence—Of the *Quantum*

Antony J. Bourdillon

UHRL, San Jose, USA
Email: bourdillona@sbcglobal.net

How to cite this paper: Bourdillon, A.J. (2022) *Harmony* Is Cause—Not Consequence—Of the *Quantum*. *Journal of Modern Physics*, **13**, 918-931.
https://doi.org/10.4236/jmp.2022.136052

Received: May 12, 2022
Accepted: June 25, 2022
Published: June 28, 2022

Abstract

Einstein claimed Bohr's theory is incomplete: "the wave function does not provide a complete description of the physical reality" [1]. Their views represent two physics in schism [2] [3]. Quanta are fundamental. The theory of diffraction in quasicrystals, that is summarized here, is falsifiable and verified. The quanta are not only harmonic; but harmonic in dual series: geometric and linear. Many have believed the quantum is real; rather than conceptual and axiomatic. The quasicrystal proves its reality.

Keywords

Quasicrystal, Icosahedra, Hierarchic, Periodic, Harmonic, Irrational, Geometric Series, Metric, Resonant Response, Dispersion Dynamics

1. Introduction

The most profound physical effect [4] that is found in a *quasicrystal* (QC), such as icosahedral Al_6Mn, is diffraction in geometric series. The effect is incompatible with Bragg's law, $n\lambda = 2d\cdot\sin(\theta)$, where diffraction in crystals occurs in integral order n; with probe wavelength λ; interplanar spacing $d = a/\left(h^2+k^2+l^2\right)^{1/2}$ in the case of a cubic crystal having lattice parameter a, and reflection indices h,k,l. In high energy electron scattering, the Bragg angle θ, is about half the scattering angle. Bragg's orders n are due to the physical harmonies that occur in 3-dimensions, at a Bragg condition, between a periodic crystal that scatters a periodic probe of photons, electrons or neutrons etc., from planes of atoms that are ordered and periodic. The order quantizes the scattering in momentum space.

By contrast, the QC was described as a "Metallic phase with long range order and no translational symmetry [5]". Part of the evidence for long range order is its sharp diffraction; and there is imaging evidence for hierarchic symmetry,

certainly in the reasonably short range of ~1500 atoms, and by indefinite extension in 3 dimensions. This symmetry is translational though not typically obvious because it occurs across planes. The 5-fold pattern of the supercluster, for example, may repeat above and below a given plane [6]. Furthermore, numeric and analytic simulations show that the probe's quasi-Bloch wave has, at the quasi-Bragg condition, translational symmetry about $a\tau^m$, and where a is the measured and calculated quasi-lattice parameter [6] [7]; where $\tau \equiv \left(1+\sqrt{5}\right)/2$ is the golden section; and m is integral.

Bragg diffraction is a quantum effect [6] in momentum space. It resembles quantized transitions between energy states in the hydrogen atom, since these states are harmonic in time and space precisely because they are spherically harmonic solutions to Schrödinger's equation. These harmonies are absent in classical, Newtonian, corpuscular physics that must be supplemented in modern physics by the wave nature of matter: the particle has a probable extension that is greater than Heisenberg's contrived uncertainty "limit" [8] and that will be simply expressed by the normal wave packet in the next section.

In 19th century physics, wave theories of light displaced Newton's corpuscular theory: in the diffraction of Huygens, Fraunhoffer and Fresnel, light diverged from motion in straight lines. In the 20th century, matter—including the electron—was found to follow similar laws but with the extra property of non zero rest mass m_o. The similarity is now indeed obvious in electron and optical microscopes. There is a third, mathematical description by axiomatic simplification and imagination, such as the notion of a point particle. Simplification is a standard route to understanding complexity, but conclusions may not be true[1]. Planck quantized Maxwell's electromagnetic wave; Bohr and Schrödinger harmonized the electronic wave. Philosophically, physics is never complete, but always falsifiable [3]. Is the quantum constitutive or a phenomenal? Is harmony its cause or consequence? Quasicrystals display complex harmonies that signify the answer.

2. Wave-Particle Duality

The facts of wave-particle duality are instances in quantum-field theory. When we include together: electromagnetism, relativity, Planck's law and the de Broglie hypothesis in the simplified units $\hbar = c = 1$ for Planck's reduced constant and the speed of light, we find simply [9]:

$$m_o^2 = \omega^2 - k^2 = (\omega + k)(\omega - k) \tag{1}$$

where ω is the wave angular velocity and k the wavevector. The functions separate conserved quantities (mass, charge, spin, energy, momentum, etc.) from elastic response waves (interference, superposition, creation, annihilation, entanglement, etc.) For a normal free particle, the functions may be expressed:

[1]Dirac did not believe truth is possible; but instead believed his theories beautiful [Pais A., in Paul Dirac, the man and his work, ed. Goddard, P., *Cambridge* (1998) ISBN 0 521 58382 9]. His was a mathematical perspective; In physics, falsification leads, by experimental elimination of competing explanations, progressively to truth [3].

$$\varphi = A \cdot \exp\left(\frac{X^2}{2\sigma^2} + X\right)$$

$$\text{with imaginary:} \quad X = i\left(\bar{\omega}t - \bar{k}x\right) \tag{2}$$

where σ depends on initial conditions that determine coherence of a packet in space and time (in manifold rank $\Re^4$) and A^2 is a normalizing constant[2]. These constants are here represented in one dimension for simplicity, but are extensible to the transverse plane with σ_y, σ_z etc. Meanwhile the angular frequencies ω and wave vectors k are in fact distributed, as represented in Equation (2) by mean values. The intensity $\phi^*\phi$ is a probability density function for a particle, or for a photon having mass $m_o = 0$. Notice that the response is elastic because its absolute, measurable value is unity: $(e^X)^* e^X = 1$, everywhere and at all time. In absence of external force, $\bar{\omega}$ and $\bar{k}$ are conserved quantities by Newton's first law of motion. For the photon, the electric and magnetic fields are real: $\boldsymbol{E} = \mathrm{Re}(\phi)$ and $\boldsymbol{B} = \mathrm{Im}(\phi)$.

The first term in the exponent of Equation (2) is Gaussian, and represents conserved properties; the second term is imaginary, so that the exponent describes an infinite wave, or field, in the complex plane (Figure 1). Of course, without the envelope function, the field amplitude is negligibly small. Some consequences of dispersion dynamics (Equation (1)) are given in **Appendix 1**.

3. Summary of Failures and Discoveries

Nowhere among the many reviews and summaries of quasicrystals in mainstream journals, is there to be found a complete description of the diffraction of this unique class of materials.

Though "long range order" is not disputed because of the sharpness of the diffraction pattern, the original claim that there is "no translational symmetry" is falsely apparent in planar images, since the symmetry is in fact three dimensional. Repetitive patterns that occur on adjacent planes can easily be simulated but not, regularly, imaged in specimen sections [6] [7].

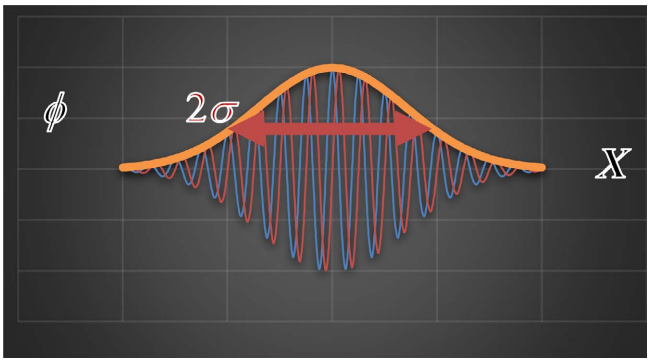

Figure 1. Normal wave packet including conservative function (orange) enveloping infinite elastic complex wave (red and blue), with uncertainty 2σ.

[2] $A^*A = \left(\int \exp\left(X^2/\sigma^2\right) \cdot \mathrm{d}\tau\right)^{-1} \cdot 2$

Because of the geometric series in the diffraction patterns, the common misconception that the phenomenon is Bragg diffraction [10] (*i.e.* in linear series) is grossly mistaken. Moreover, attempts to describe the pattern have generally employed six unexplained dimensions, *i.e.* "multiplied without necessity". Without the proper explanation for the geometric series diffraction, the widespread obsession with Penrose tiling is confused, misguided and inconsequential.

All of these failures are overcome by the hierarchic model (**Figure 2**). This has been systematically published in several monographs and multiple, refereed articles in scientific journals e.g. [6] [11] [12] [13]. The explanation is consistent, verified, and, in essentials, complete.

In summary:

The unit cell is consistent with imaging scales: it contains a central *Mn* atom surrounded by 12 *Al* atoms, icosahedrally coordinated. It is extremely dense.

The atoms and cells are hierarchically arranged in geometric spatial order.

The model is infinitely extensive, uniquely aligned from cell to cell, and uniquely icosahedral except for minor fillings with interstitial atoms or structures. The fillings occur because the cells are edge sharing and not strictly space filling as are the cells in crystals. Nevertheless the fillings contain a small and negligible percentage (~2%) of the bulk volume.

In the absence of Bragg diffraction, the patterns are successfully indexed in 3 spatial dimensions, including both stereographic axes (**Figure 2(c)**) and the diffraction planes [14] that are normal to them. Dimensions should not be multiplied without necessity.

In a further major break from Bragg diffraction, the indexation of axes and planes occurs generally in irrational and geometric orders.

Whereas the diffraction is not Bragg diffraction, so that relationships between wavelength, order, interplanar spacing and scattering angle are *a priori* undefined; nevertheless, the structure factor method can be used to simulate the QC diffraction. This is because the method is *a priori* independent of scattering angle, and so has an extra degree of freedom. This freedom is critical.

Again, in the absence of Bragg diffraction, the scattering has been accurately simuated by modified structure factors. Two modifications are introduced into the Quasi-Structure-Factor calculations (**Appendix 2**, **Figure 3**):

Firstly a coherence factor c_s is introduced to account for the multiple interplanar spacings that occur in diffraction from hierarchic icosahedral structure and verified in imaging. (By contrast, crystallography assumes unique d for each Bragg beam.)

Secondly, because the cells are not linearly periodic, the normal summations are made over a whole quasicrystal of given order; not just over a unit cell as is the practice of crystallography.

The calculations have proved, surprisingly, high coherence of the scattering from the hierarchic model, with line widths a small fraction of the corresponding quasi-Bragg angle ($\sim 10^{-4}$) in a supercluster order 6, having about 10^8 atoms) [6] [10] [15].

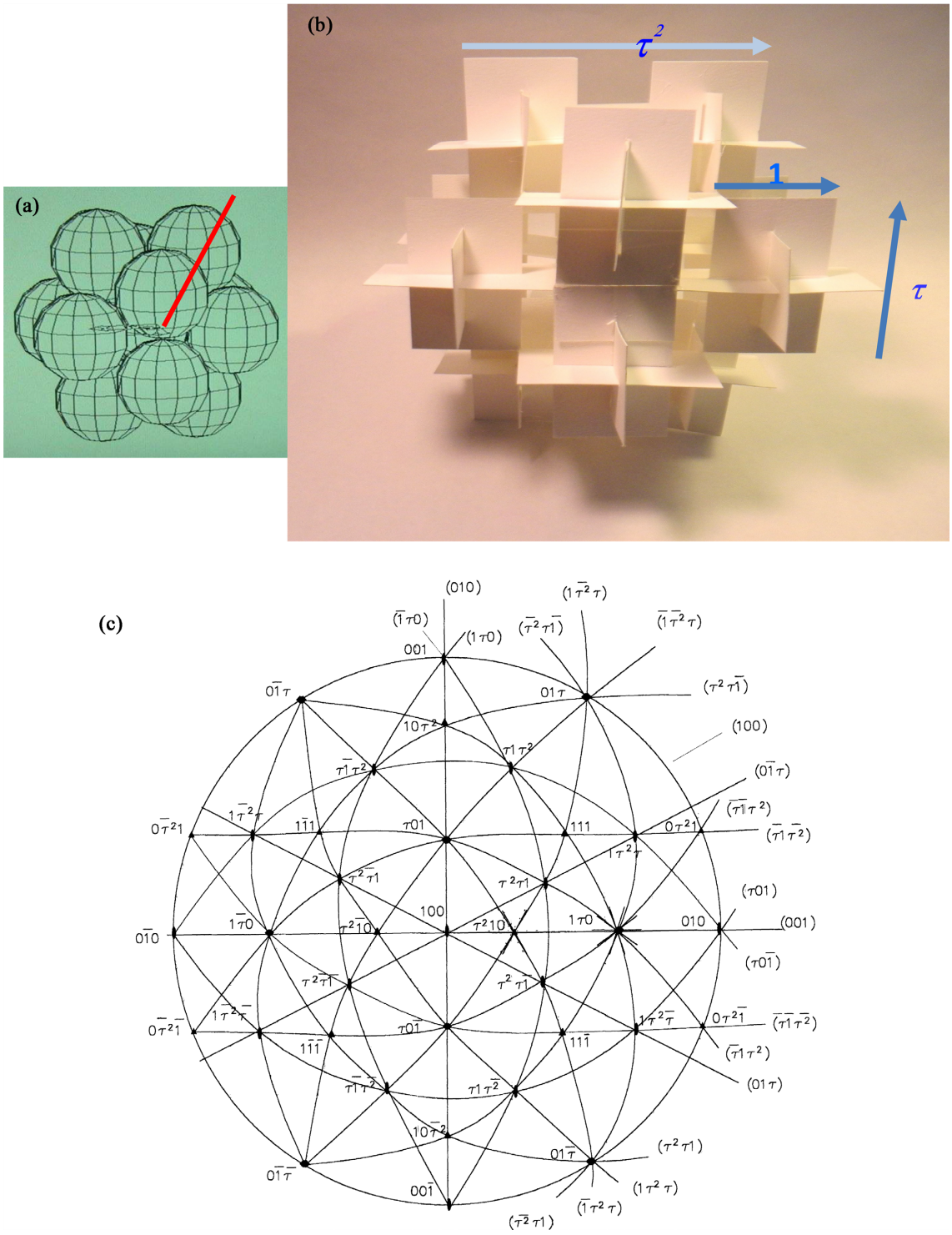

Figure 2. (a) Icosahedral unit cell with central *Mn* atom and 12 *Al* atoms. Notice 5-fold axis (red) normal to two circles of 5 *Al* atoms. Ten cells, covering two circles, is a typical cluster group in imaging [6]. The cell is extremely dense. (b) Hierarchic icosahedral structure. Notice the stretching factor (τ^2) from the unit cell (side width 1 × length τ) to cluster ($\tau^2 \times \tau^3$). (c) Stereogram of the principal axes for the icosahedral structure. Normal to them are the principal diffraction planes. They are all 3-dimensional with indices τ^m where the golden section $\tau = \left(1+\sqrt{5}\right)/2$. After William of Ockham, "Dimensions should not be multiplied without necessity." All of the beam intensities in the original data [5] have been indexed and calculated [11].

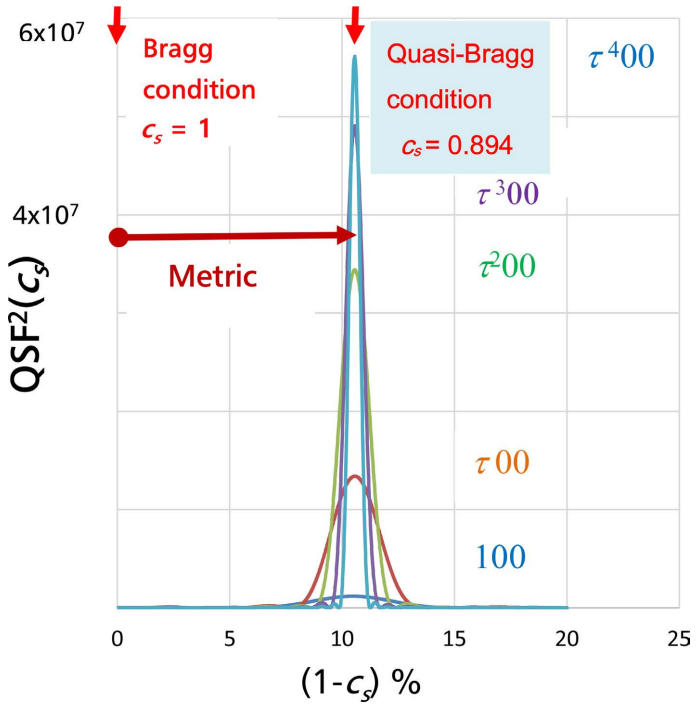

Figure 3. Quasi structure factors (supercluster order $p = 2$) calculated (**Appendix 2**) by scanning for five peaks in geometric sequence against the coherence factor c_s. At $c_s = 1$, there is no Bragg diffraction, the same quasi-Bragg condition occurs at $c_s = 0.894$ for *all* diffracted beams. Geometric series indices are shown level with the tops of corresponding QSF peaks. Intensities match experiments.

The diffraction from the hierarchic structure model accurately simulates recorded diffraction pattern intensities.

The coherence factor shifts the scattering angle (double the Bragg angle) by a factor that is the same throughout *all beams in all diffraction patterns*. Knowledge of the factor is essential in measurement and verification.

The factor has been analysed to an accuracy of 3 figures. Given the 3-dimensional indexation in geometric and irrational series, it is possible to separate the irrational part from an approximate natural part that is Bragg-like ($c_s = 1$). The irrational residue forms a metric function that is identical for all indexations and all orders of beams in the diffraction pattern. *The analytic function is the exact inverse of the scattering factor that was introduced in the QSF method and simulated numerically*. This discovery is extraordinary and highly significant in the explanation for diffraction in QCs.

The proof of both c_s value and general understanding, that is obtained by exactly matching numerical and analytic methods, verifies the new Quasi-Bragg law for this icosahedral solid:

$$\tau^m \lambda = 2d' \cdot \sin\left(\theta / c_s\right) \tag{3}$$

where the quasi-Bragg angle is larger than the corresponding Bragg angle by the factor $1/c_s$ after taking also into account the geometric orders instead of linear n. In 3-dimensions, $\boldsymbol{m}$ and $\boldsymbol{d'}$ are correspondingly vectorial.

The success in understanding the coherence factor, enables verification of the model and theory by measurement: the quasi-lattice-parameter, measured by standard methods that are modified to apply to QSFs, is the same as the known diameter of *Al* atoms, as indeed it must be under the model (**Table 1**, **Figure 4**, **Appendix 3**).

This hierarchic model is adaptable to space filling by interstial defects. The general structure is that of quasi-spheres of multiple order that are densely packed, each sphere being identically oriented by sharing of multiple icosahedral edges.

Table 1. Comparison between Bragg and quasi-Bragg optics.

Bragg	Quasi-Bragg	Comment
$n\lambda = 2d\sin(\theta)$	$\tau^m\lambda = 2d'\sin(\theta')$	Harmonic laws Give $\theta' = \theta/c_s$
$S_{hkl} = \Sigma f_i \cos(2\pi \boldsymbol{h}_{hkl}\cdot\boldsymbol{r}_i)$	$S'_{hkl} = \Sigma f_i \cos(2\pi c_s \boldsymbol{h}_{hkl}\cdot\boldsymbol{r}_i)$ Including iterations (**Appendix 2**)	q-Structure factors Give c_s, a' and d'
$d = a/h$	$d' = ac_s\tau$	$d = a\left(h^2+k^2+l^2\right)^{-1/2}$ $d' = dc_s$
hastily Measured a $a = 0.205$ nm	Corrected measurement $a' = 0.29$ nm (**Appendix 3**)	Measured quasi-lattice-parameter 0.29 nm = dia(Al)

n: Bragg order; S_{hkl}: Structure factor; λ: wavelength; f_i: atomic scattering factor for atom i; d: interplanar spacing; c_s: coherence factor; θ: Bragg angle; $\boldsymbol{r}_i$: location of atom i; τ: golden section; $\boldsymbol{h}_{hkl}$: normal to (hkl) plane; Prime: hierarchic equivalent; a: lattice parameter.

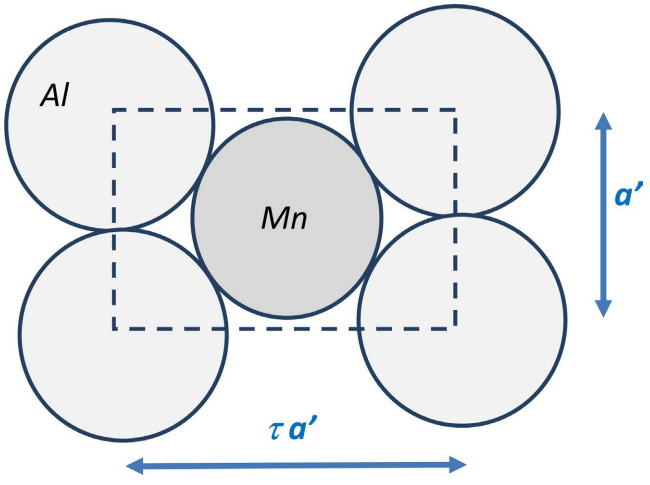

Figure 4. Golden-rectangle cross-section of the icosahedral unit cell in i-Al_6Mn, having side width a' (the quasi-lattice parameter) and length $\tau a'$. The unit cell contains 15 identical sections at various orientations. It is therefore quasi-spherical. This unit cell is extremely dense and depends on atomic diameter ratios $d_{Mn}/d_{Al} = \sqrt{1+t^2} - 1$.

4. Dual Harmonies in Diffraction That Occurs in Irrational and Geometric Order

Further illustration with quasi-Bloch waves in QCs at the quasi-Bragg condition, illustrates consequences of the irrational QC diffraction (**Figure 5**). In a crystal oriented to a first order Bragg condition an advancing electron beam interacts with the reflecting lattice to form two momentum dispersed Bloch bands. Their relative intensities depend on specimen thickness; on orientation; and they form regular fringes in wedge foils; and lattice images in high resolution imaging [16]. The fringes are commensurate with the unit cell and with all cells periodically repeating as represented in the blue wave of the figure. However, these Bloch waves are incommensurate with the hierarchic quasi-lattice that is geometric and irrational. When the scale is multiplied by the metric function (**Table 2**) [17];

$$\frac{1}{c_s} = 1 + \frac{\tau^m - F_{m+4}/2}{F_{m+1}} = \frac{1}{0.894} \tag{4}$$

the (red) wave becomes commensurate with the geometric quasi-lattice both long range, and at linear short range on each geometric intercept, *i.e.* all *m*. In equation 4, F_m represents the Fibonacci sequence base (0, 1). The quasi-Bloch wave is translationally invariant about all geometric intercepts $a\tau^m$. Notice that the spacings between intercepts are in Fibonacci series that are represented by the denominator in Equation (4), F_{m+1}.

Most Important is the fact that the quasi-Bloch wave is dual harmonic. The irrational part of any index is represented by the fraction in the metric function and this digitizes the periodic probe onto the hierarchic lattice while effectively decreasing the quasi-d-spacing by c_s. The dual harmony enables the periodic probe to scatter coherently from the hierarchic lattice into a geometric reciprocal lattice with a peculiar and precise quasi-lattice constant.

It is obvious that the dual harmony forces the quantization of the quantized

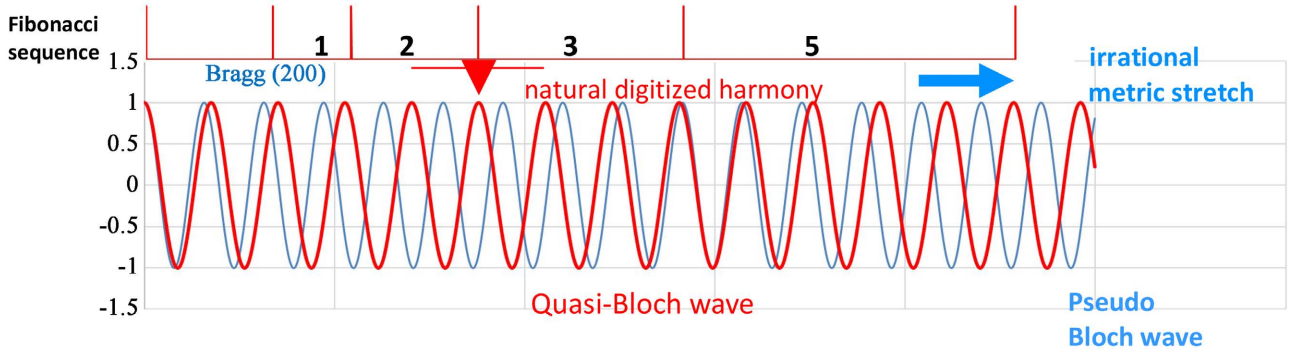

Figure 5. Crystalline Bloch waves (blue) are commensurate with their unit cell and corresponding periodic crystal lattice at the Bragg condition. When this wave is stretched horizontally by the inverse coherence factor $1/c_s$, the quasi-Bloch-wave (QBW in red) commensurates with the irrational, geometric and hierarchic, quasi-lattice. Its geometric order is represented by the intercepts on the horizontal line above it. The digitized number of periodic cycles between successive intercepts is in Fibonacci sequence (denominator in Equation (4)), and the diffraction is logarithmically periodic. The natural and irrational parts of the indices are separable: the irrational part is expressed by the metric stretch; the natural part scatters with sharp, coherent diffraction.

Table 2. Analytic solution for the metric function. Irrational parts are colored red. F_m represents mth term (m = 0,1,2,⋯) of Fibonacci sequence on bases in brackets. Delta is the Dirac function. The metric function is (1 + irrational residue), and is the same for all m. The analytic solution is identical to the numeric QSFs to three figures.

Fact:		τ^m	=	$F_m(1, \tau)$	=	$\partial_{(m,1)}$	+	$F_{m-1}(0, 1)$	+	$F_m(0, 1)\tau$
$\partial + F_{m-1}$	+	$F_m\tau$	=	τ^m		m	=	0, 1, 2, 3, ⋯		
1	+	0	=	τ^0						
0	+	τ	=	τ^1						
1	+	τ	=	τ^2						
1	+	2τ	=	τ^3						
2	+	3τ	=	τ^4						
3	+	5τ	=	τ^5	=	$F_4(01)$	+	$F_5(0, 1)\tau$ approx	=	$F_5(1, \tau)$
Approx				τ^m	−	$F_{m-1}(01)$	−	$F_m(01)\frac{3}{2}$	=	residue
Metric	fn	:	{	$1+(\tau^m$	−	$F_{m+4}/2$	)	$/F_{m+1}\}$	=	$1/c_s$

momentum that is evident in the diffraction pattern. *It is reasonable to make the hypothesis that all quantization is the result of—not the cause of—harmonic dynamic variables*. Further confirmation may, in future, be found from multi-slice calculations of quasi-Bloch wave intensities as probe interacts with specimen. This becomes more feasible now that c_s is known and understood and applied with geometric, band-gap potentials [18].

More generally it follows that since "matter tells space how to curve" while "space tells matter how to move", then, without harmony, quantization of the graviton is a profoundly problematic notion until a harmonius wave can be identified.

5. Discussion

It is not enough for mainstream (self-styled) quasicrystallographers to fail over a period of 40 years to describe the physics of geometric series diffraction, while at the same time to censor the correct solution by unscientific quasi-reasoning (e.g. [15] pp. 89-109).

The diffraction requires dual harmonies: one long range; the other short. That this happens proves that the dual harmony determines, and ranks higher than, the quantum that they produce. The importance of this result is that it shows that mathematical axiomatization of the quantum is not a complete representation of the physics; nor is a common fixation on small spaces and quantities. Large scale bridges resonate as atoms do and this is the unified basis of modern physics. The realism we share with Einstein [19].

6. Conclusions

Our exact match between analytic and numeric calculations for the coherence factor justifies the following conclusions. Quantization is a mathematical device that, in physics, applies only to harmonic entities. If gravity is not harmonic around matter there is little reason, in physics, for the graviton to exist. Where material wavefunctions are harmonic—in the H atom, nuclear particles etc.—then obviously, by Newton's law of gravitation and Einstein's general relativity, gravity is quantized by the quantized masses.

We wonder why for so long, mainstream QC theory failed to explain geometric diffraction? Momentum quanta cause the sharp diffraction in dual short range and long range. After Planck discovered the quantum in the photoelectric effect, and before Schrödinger quantized the basis states of the hydrogen atom, Bragg demonstrated crystal diffraction wherein momentum changes, ordered by integral n, are quantized by harmonic interference between periodic crystal planes. This diffraction is due to harmonic interactions in space and time. Now we find that quasicrystals diffract, uniquely, with dual harmonies in both geometric and periodic series. The quantum is therefore second fiddle to harmony: as consequence to cause.

Conflicts of Interest

The author declares no conflicts of interest regarding the publication of this paper.

References

[1] Einstein, A., Podolski, B. and Rosen, N. (1935) *Physical Review*, **47**, 777-780. https://doi.org/10.1103/PhysRev.47.777

[2] Popper, K. (1982) Quantum Theory and the Schism in Physics. Hutchison, London.

[3] Popper, K. (1980) The Logic of Scientific Discovery, Schism in Physics. Hutchison, London.

[4] Popper, K. (1982) The Open Universe, an Argument for Indeterminism. Hutchison, London.

[5] Shechtman, D., Blech, I., Gratias, D. and Cahn, J.W. (1984) *Physical Review Letters*, **53**, 1951-1953. https://doi.org/10.1103/PhysRevLett.53.1951

[6] Bourdillon, A.J. (2021) *Journal of Modern Physics*, **12**, 1618-1632. https://doi.org/10.4236/jmp.2021.1212096

[7] Bourdillon, A.J. (2021) *Journal of Modern Physics*, **12**, 1012-1026. https://doi.org/10.4236/jmp.2021.127063

[8] Bourdillon, A.J. (2020) *Journal of Modern Physics*, **11**, 365-377. https://doi.org/10.4236/jmp.2020.113023

[9] Bourdillon, A.J. (2012) *Journal of Modern Physics*, **3** 290-296. https://doi.org/10.4236/jmp.2012.33041

[10] Steurer, W. (2004) *Zeitschrift für Kristallographie*, **219**, 391-446. https://doi.org/10.1524/zkri.219.7.391.35643

[11] Bourdillon, A.J. (2011) Logarithmically Periodic Solids. Nova Science, Hauppauge.

[12] Bourdillon, A.J. (2009) Quasicrystals and Quasi Drivers.

[13] Bourdillon, A.J. (2022) Further Evidence Is Listed in Publications in. https://www.xraylithography.com

[14] Bourdillon, A.J. (2013) *Micron*, **51**, 21-25. https://doi.org/10.1016/j.micron.2013.06.004

[15] Bourdillon, A.J. (2012) Metric, Myth and Quasicrystals. UHRL, San Jose.

[16] Hirsch, P., Howie, A., Nicholson, R.B., Pashley, D.W. and Whelan, M.J. (1977) Electron Microscopy of Thin Crystals. Krieger, New York.

[17] Bourdillon, A.J. (2020) *Journal of Modern Physics*, **11**, 581-592. https://doi.org/10.4236/jmp.2020.114038

[18] Bourdillon, A.J. (2010) Quasicrystals' 2D Tiles in 3D Superclusters. UHRL, San Jose.

[19] Pais, A. (1991) Niels Bohr's Times in Physics, Philosophy and Polity. Clarendon, Oxford, 433.

[20] Bourdillon, A.J. (2018) *Journal of Modern Physics*, **9**, 1304-1316. https://doi.org/10.4236/jmp.2018.96079

[21] Bourdillon, A.J. (2018) *Journal of Modern Physics*, **9**, 2295-2307. https://doi.org/10.4236/jmp.2018.913145

[22] Bourdillon, A.J. (2020) *Journal of Modern Physics*, **11**, 1926-1937. https://doi.org/10.4236/jmp.2020.1112121

[23] Bourdillon, A.J. (1987) *Philosophical Magazine Letters*, **55**, 21-26. https://doi.org/10.1080/09500838708210435

[24] Tsai, A.P. (2008) *Science and Technology of Advanced Materials*, **9**, 1-20. https://doi.org/10.1088/1468-6996/9/1/013008

Appendix 1. Dispersion Dynamics

Differentiation of Equation (1) provides the equations for dispersion dynamics in simplified units, including:

$$\frac{\omega}{k}\cdot\frac{\mathrm{d}\omega}{\mathrm{d}k}=1 \tag{A.1}$$

where the normalized phase velocity of the wave $v_p/c = \omega/k$. The integrated beat velocity in Equation (2) is the normalized group velocity, $v_g/c = \mathrm{d}\omega/\mathrm{d}k$, as follows: consider two tuning forks, off pitch with frequencies $\omega \pm \Delta\omega/2$. The frequencies with mean phase frequency ω; beat as waves that continuously construct and destruct. Their beat varies in time with frequency $\Delta\omega$. Likewise, the phase and beat wavevectors are k and Δk respectively, since generally $k = 2\pi/\lambda$, where λ is wavelength. The beat velocity is therefore $\Delta\omega/\Delta k$. Then summing $\Delta\omega$ over all frequencies in Equation (2), reveals the group velocity since $v_p \cdot v_g = c^2$ is constant in the theory of relativity. This relationship is the same for massless photons as for massive particles. In special relativity $v_g \le c$ and this is the velocity of reference frames; while, in vacuo, $v_p \ge c$. The wave is elastic and does not carry energy. Energy, like momentum, is described by the conserved envelope function.

Equation A.1 has many consequences. Notice that Equation (2) linearizes the second order equation 1 of special relativity, and so they perform a similar function for the free particle that Dirac's equation serves for the bound electronic states in an atom. Moreover the equations 1 separate the propagation direction from transverse directions and this has many consequences including: solutions for negative mass [20][3], phase velocity [7], uncertainty, Newton's second law, electron spin (as resistanceless paramagnetism in phase space, that is consistent with Hundt's rules in atomic structure), intrinsic magnetic radius [21] and fine structure constant, reduction of the wave packet, [22] etc. The equations apply in harmonius diffraction by quasicrystals and crystals, as they do in the time independent Schrödinger equation that operates on steady-state harmonic bases. The diffraction orders and quantum numbers respectively describe interaction requirements that are quantized by *necessary constructive interference over space and time.* The formalism in Equation (2) enables our understanding of the fundamental interaction required in the coherent diffraction in QCs as described above.

In particular, the mystery in Planck's law that was discovered in photons, is that—for each independent photon—the energy is quantized and is therefore equal to the integral $\int \varepsilon\varepsilon_0 \boldsymbol{E}^2/2 + \mu\mu_0 \boldsymbol{B}^2/2\,\mathrm{d}x\cdot\mathrm{d}y\cdot\mathrm{d}z = \hbar\omega$ (where $\varepsilon\varepsilon_0$ is the medium's electric permittivity and $\mu\mu_0$ its magnetic permeability). The fact was a synthetic proposition, empirically discovered. It compares with equations 2 from which densities $\int c^2\cdot\rho\left(\phi^*\phi\right)\mathrm{d}x\cdot\mathrm{d}y\cdot\mathrm{d}z = 1\cdot mc^2$, which is also quantized and analytic. However, in the quasicrystal the quantized changes in momentum Δp

[3]To avoid unphysical singularities in v_g and v_p when $k = -m_o$ in the antiparticle, the switching principle is switched back [8]; the antiparticle mass is switched instead.

that occur in diffraction are in no way mysterious; but are necessitated by dual harmony and constructive interference. This quantization is both synthetic and analysed[4].

Appendix 2. Quasi-Structure-Factor (QSF)

Since quasicrystals do not obey Bragg's law of diffraction, nothing is known *a priori* about corresponding relationships between θ', λ and d'. However, the *structure factor* (SF) method is independent of θ: we can use the method by applying the known relationship between interplanar spacing d and the index h_{hkl} in the case of crystalline cubic symmetry: $d = a/\sqrt{h^2+k^2+l^2}$. Here a represents the lattice parameter, and subscripts h, k and l represent the 3-dimensional indices in the diffraction pattern [12] [15]. It turns out (e.g. **Figure 4**) that all structure factors in the quasicrystal are zero. The implied absence of diffraction should be expected in a solid whose images demonstrate multiple interplanar atomic spacings. However it turns out further, that by introducing a coherence factor c_s, specific to the *hierarchic icosahedral* (HI) structure, a quasi-Bragg condition is discovered that is as sharp as the Bragg condition commonly observed by rocking crystals. The coherence factor is discovered by simulations in which the factor is numerically scanned while evaluating the QSF, first by summing over the unit cell with atomic scattering factors $f_i = f_{\mathrm{Al,Mn}}$ in Equation (A.2), and secondly over clusters order $(p-1) \geq 0$, by iteratively adding cluster centers at $\boldsymbol{r} = \boldsymbol{r}_{cc}$ in equation A.3 [6]:

$$S_{hkl} = \Sigma_i^{\mathrm{Al,Mn}} f_i \cos\left(2\pi \cdot c_s \left(\boldsymbol{h}_{hkl} \cdot \boldsymbol{r}_i\right)\right) \tag{A.2}$$

$$S_{hkl}^{p} = S_{hkl}^{p-1} \cdot \Sigma_{cc} \cos\left(2\pi \cdot c_s \tau^{2p} \left(\boldsymbol{h}_{hkl} \cdot \boldsymbol{r}_{cc}\right)\right) \tag{A.3}$$

All atoms scatter.

In crystals by contrast, the SF is simpler and is represented by equation A.2 with simulated $c_s = 1$. There, the calculation is comparatively easy because the summation is limited to one unit cell that repeats periodically. Symmetry in the unit cell often forces $S_{hkl} \to 0$, or to a small range of values. In quasicrystals, by contrast, the QSFs are calculated over all the atoms in a selected order of HI after scanning for optimum c_s (**Figure 3**). The QSFs contain a spectrum of amplitudes whose corresponding intensities match experimental beam intensities reasonably well [15].

Under the quasi-Bragg law, $d' = a'/\sqrt{h^2+k^2+l^2}$. The quasi-lattice parameter is calculated on the $(\tau 00)$ reflection, since it is the strongest line in the five fold axial pattern and corresponds to both the length of the unit cell and the typical separation of unit cells, is $a' = a \cdot c_s \cdot \tau$, where (unprimed) a was previously calculated under the false assumption of Bragg diffraction [23] [24] and a' is the (unit) width of the quasicrystal unit cell (**Figure 4**).

[4]In two independent steps: experimental *a posteriori* and theoretic *a priori*.

Appendix 3. Verification of Quasi-Lattice-Parameter a'

Bragg's law of crystal diffraction is written $n\lambda = 2d\sin(\theta)$.

In cubic crystals, $d = a/\left(h^2 + k^2 + l^2\right)^{1/2}$. This formula applies in part to the quasicrystal because O_8 is a subgroup of the icosahedral point group symmetry. This fact provides advantage in 3-dimensional, Euclidean indexation.

The quasi-Bragg law of diffraction should be written $\tau^m\lambda = 2d'\sin(\theta')$. Here, indices (Table 2) are separable into natural and irrational parts. Simulations of imaginary structures that have the following basis in the natural approximation $\tau^m \to \partial_{(m,1)} + F_m(01) + F_{m+1}(01)\frac{3}{2}$, show such concepts to be Bragg-like with c_s= 1. They actually have multiple peaks because of misalignment of cells, but the conclusion is simple: there is a change in scattering angle due to the irrational residue. Optical considerations show $\theta' = \theta/c_s$, and this is confirmed by simulations.

It follows from a comparison of Bragg's law with the quasi-Bragg law that $d' = dc_s$ and therefore that $a' = ac_s$. There is however a further complication: the line that we used to "measure" the lattice parameter shown in Table 1, column 1, row 5 is the indexed line (τ00). This is because it belongs to the "third bright ring" in Shechtman's data [5] which was mysterious at the time. In axial diffraction patterns it is normal for brightness to fall on beams away from the central (000) zero order beam owing to increasing deviation parameter [16]. However, the quasicrystal is not so simple: the reason why the third ring is bright is because it corresponds to the length of the unit cell and also the typical distance between unit cells in the hierarchic structure. This ring is also brightest in simulations, regardless the deviation parameter.

The further correction is thus: $a'_{(100)} = a_{(\tau 00)}c_s\tau$ *i.e.* correcting for the index in line 2 of this appendix. Then $a' = 0.29$ nm as on Table 1, column 3, row 5. The quasi-lattice-parameter is the same as the diameter of the Al atoms in Figure 4. This is a necessary form of verification in normal crystallography.